Published in final edited form as:
Neuroimage. 2009 August 15; 47(2): 459–466. doi:10.1016/j.neuroimage.2009.04.060.

DTI abnormalities in anterior corpus callosum of rats with spike-wave epilepsy

H. Chahboune, PhD[1,2,3], **A.M. Mishra, PhD**[4], **M.N. DeSalvo, BS**[4], **L.H. Staib, PhD**[3,5], **M. Purcaro, MS**[4], **D. Scheinost, BA**[1,2,3,5], **X. Papademetris, PhD**[1,2,3,5], **S.J. Fyson, BSc**[6], **M.L. Lorincz, PhD**[6], **V. Crunelli, PhD**[6], **F. Hyder, PhD**[1,2,3,5], and **H. Blumenfeld, MD, PhD**[1,2,4,7,8]

[1]Magnetic Resonance Research Center (MRRC), Yale University School of Medicine, 333 Cedar Street, New Haven, Connecticut 06520, USA

[2]Core Center for Quantitative Neuroscience with Magnetic Resonance (QNMR) Yale University School of Medicine, 333 Cedar Street, New Haven, Connecticut 06520, USA

[3]Department of Diagnostic Radiology, Yale University School of Medicine, 333 Cedar Street, New Haven, Connecticut 06520, USA

[4]Department of Neurology, Yale University School of Medicine, 333 Cedar Street, New Haven, Connecticut 06520, USA

[5]Department of Biomedical Engineering, Yale University School of Medicine, 333 Cedar Street, New Haven, Connecticut 06520, USA

[6]School of Biosciences, Cardiff University, Museum Avenue, Cardiff CF10 3AX, UK

[7]Department of Neurobiology, Yale University School of Medicine, 333 Cedar Street, New Haven, Connecticut 06520, USA

[8]Department of Neurosurgery, Yale University School of Medicine, 333 Cedar Street, New Haven, Connecticut 06520, USA

Abstract

Objective—Absence epilepsy is a common seizure disorder in children which can produce chronic psychosocial sequelae. Human patients and rat absence models show bilateral spike-wave discharges (SWD) in cortical regions. We employed diffusion tensor imaging (DTI) in rat absence models to detect abnormalities in white matter pathways connecting regions of seizure activity.

Methods—We studied Wistar albino Glaxo rats of Rijswijk (WAG/Rij), genetic absence epilepsy rats of Strasbourg (GAERS), and corresponding nonepileptic control strains. *Ex vivo* DTI was performed at 9.4T with diffusion gradients applied in 16 orientations. We compared fractional anisotropy (FA), perpendicular ($\lambda\perp$) and parallel ($\lambda_{\parallel}$) diffusivity between groups using t-maps and region of interest (ROI) measurements.

Results—Adult epileptic WAG/Rij rats exhibited a localized decrease in FA in the anterior corpus callosum. This area was confirmed by tractography to interconnect somatosensory cortex regions most intensely involved in seizures. This FA decrease was not present in young WAG/Rij rats before onset of SWD. GAERS, which have more severe SWD than WAG/Rij, exhibited even more pronounced callosal FA decreases. Reduced FA in the epileptic animals originated from an increased $\lambda\perp$ with no significant changes in $\lambda_{\parallel}$.

Correspondence to: Hal Blumenfeld, MD, PhD, Yale Depts. Neurology, Neurobiology, Neurosurgery, 333 Cedar Street, New Haven, CT 06520-8018, Tel: 203 785-3928 Fax: 203 737-2538, Email: E-mail: hal.blumenfeld@yale.edu.

Interpretation—Reduced FA with increased $\lambda\perp$ suggests that chronic seizures cause reduction in myelin or decreased axon fiber density in white matter pathways connecting regions of seizure activity. These DTI abnormalities may improve the understanding of chronic neurological difficulties in children suffering with absence epilepsy, and may also serve as a noninvasive biomarker for monitoring beneficial effects of treatment.

Introduction

Absence seizures affect 10–15% of children with epilepsy, and can significantly impair quality of life. Onset is typically at age 5–7 years, with frequent staring spells and spike-wave discharges (SWD) on electroencephalography (EEG). There is also milder impaired attention between absence episodes (Levav et al., 2002;Mirsky and Van Buren, 1965), and long-term psychosocial sequelae are not uncommon (Camfield and Camfield, 2002;Wirrell et al., 1997). Improved noninvasive methods are needed to study the long-term consequences of this disorder, to better understand the pathophysiology, and to investigate potential beneficial effects of treatment.

Previous studies suggest that typical SWD in absence epilepsy depend on long-range cortico-thalamic and cortico-cortical network interactions (Avoli and Gloor, 1982;Blumenfeld, 2005;Blumenfeld and McCormick, 2000;Meeren et al., 2005). Although considered “generalized” (ILAE, 1981), there is substantial evidence that specific networks are intensely involved in absence epilepsy, while others are spared (Blumenfeld, 2003,2005). On human EEG, SWD amplitude is typically greatest in midline frontal regions, and smaller in occipital regions (Holmes et al., 2004;Rodin and Ancheta, 1987;Weir, 1965). Numerous fMRI studies of patients with spike-wave epilepsy have also shown changes in bilateral cortex and thalamus during SWD (Archer et al., 2003;Berman et al., 2008;Gotman et al., 2005;Hamandi et al., 2008;Moeller et al., 2008). The corpus callosum is a crucial conduit for synchronizing intense SWD activity in the two hemispheres, since cutting the corpus callosum in rodent and feline models of absence leads to independent SWD on the left and right without contralateral synchrony (Musgrave and Gloor, 1980;Vergnes et al., 1989). Given the importance of network interactions in SWD generation, we expected that neuroimaging methods geared towards networks would be particularly well suited to measuring chronic structural brain abnormalities in this disorder.

Investigation of the corticothalamic networks crucial to SWD generation have been greatly enhanced by a number of experimental animal model systems (Avoli et al., 1990;Crunelli and Leresche, 2002). Rodent models, such as Wistar albino Glaxo rats of Rijswijk (WAG/Rij rats), and the genetic absence epilepsy rats from Strasbourg (GAERS), resemble the human disorder in behavior during seizures, EEG, and response to medications (Coenen et al., 1992;Danober et al., 1998). Like in humans, investigation of these models has shown bilateral cortical involvement during SWD. Thus, numerous electrophysiological, fMRI, and molecular studies have demonstrated intense involvement of the anterior brain perioral and barrel (S1BF) somatosensory cortex, while occipital cortex is almost entirely spared during seizures (Klein et al., 2004;Meeren et al., 2002;Nersesyan et al., 2004a;Nersesyan et al., 2004b;Vergnes et al., 1990).

Animal models have also been important for recent investigations of the beneficial effects of early treatment on spike-wave epilepsy. We found that early treatment of a genetic rat absence model can improve the phenotype, reducing seizures and preventing long-term molecular changes associated with this disorder (Blumenfeld et al., 2008). These findings raised the hope that as the genetics of absence epilepsy becomes better understood, it will be possible to predict the risk of this disorder, and improve outcome through early therapeutic intervention. To implement this treatment approach, it will be necessary to develop non-invasive biomarkers,

first in animal models, and ultimately in human treatment trials, to monitor long-term microstructural changes in the brain associated with the abnormal phenotype and its prevention by treatment.

Several imaging approaches have been used to measure chronic changes in idiopathic generalized epilepsy, including MR spectroscopy and morphometric analysis (Bernasconi et al., 2003;Chan et al., 2006;Duncan, 2004, 2005;Woermann et al., 1998). However, these imaging approaches have not emphasized the network dysfunction known to play a critical role in the generation of SWD (Avoli et al., 1990;Blumenfeld, 2005;Crunelli and Leresche, 2002). Diffusion tensor imaging (DTI) provides a method for assessing the microstructural integrity of long-range white matter networks, based on the diffusion properties of water in tissue (Basser and Jones, 2002;Chahboune et al., 2007;Kale et al., 2006;Mori and Zhang, 2006). DTI has emerged as a useful tool for measuring subtle white matter changes in numerous disease states including Alzheimer's disease, multiple sclerosis, stroke, schizophrenia and others (Assaf and Pasternak, 2008;Boska et al., 2007;Budde et al., 2007;DeBoy et al., 2007;Mori et al., 2002;Song et al., 2004). In epilepsy, DTI has also found growing use in both human patients (Eriksson et al., 2001;Grant, 2005;Kimiwada et al., 2006;Luat and Chugani, 2008;Rugg-Gunn et al., 2001;Rugg-Gunn et al., 2002;Thivard et al., 2005) and in animal models (Obenaus and Jacobs, 2007) by identifying potentially epileptogenic lesions, providing information about pathways for seizure propagation, and detecting abnormalities even when conventional MRI is normal. In this study, we have therefore used DTI in the WAG/Rij absence rodent model at two different developmental stages, before and after the onset of epilepsy to first identify DTI changes related to epileptogenesis. We then used a different animal model of absence (GAERS) to determine the specificity of these changes. These *ex vivo* DTI results in spike-wave epilepsy models are an important step for understanding neurological difficulties in children suffering from absence epilepsy, demonstrating that white matter abnormalities could contribute to chronic dysfunction in what has classically been considered a gray matter disorder. In addition, this approach may be useful for developing noninvasive methods to evaluate potential beneficial effects of early treatment.

Methods

Animals

All procedures were in full compliance with approved institutional animal care and use protocols. Animals studied were female Wistar albino Glaxo rats of Rijswijk (WAG/Rij) ((Harlan, Indianapolis, Indiana, USA) at 1.7 and 8 months and age-matched nonepileptic (control) Wistar rats from Charles River Laboratories (Raleigh, NC, USA), as well as female genetic absence epilepsy rats of Strasbourg (GAERS) and its nonepileptic control (NEC) (both strains bred at Cardiff University, originating from Strasbourg) at 4.2 months. GAERS have a mature SWD phenotype by about 2 months of age, while WAG/Rij rats have fully developed SWD by about 4 months (Depaulis and van Luijtelaar, 2005), so both the adult WAG/Rij and adult GAERS groups exhibited fully developed SWD at the time of the experiment. Six groups of animals were studied: adult WAG/Rij (n= 9), adult Wistar control (n= 7), young WAG/Rij (n=6), young Wistar control (n=5), adult GAERS (n=5), adult NEC (n=5). To match conditions for recording, perfusion, and imaging (Kim et al., 2007), all procedures were performed in parallel in age-matched epileptic and non-epileptic animals.

Electrode implantation

For WAG/Rij and nonepileptic Wistar controls, under ketamine (100mg/kg), xylazine (10mg/kg), and acepromazine (1mg/kg) anesthesia, we implanted stainless steel tripolar electrodes (Part # MS333/3-A, Tripolar electrode uncut untwisted 0.005; Plastics One Inc., Roanoke, VA; Internal control # 8LMS3333XXXE, Pedestal Height: 8 mm.) using a stereotactic frame (David

Kopf Instruments, Tujunga, CA). To provide good electrical contact before wrapping around skull screws, the ends of the recording electrodes were prepared by scraping off all the polyimide insulation and exposing stainless steel wire up to 10 mm from the tip, leaving insulation intact proximally, as verified under the microscope. Level of anesthesia was monitored by respiration, heart rate, glabrous skin perfusion, and response to foot pinch. Small burr holes (using Micro Drill Steel Burrs, 2.3mm shaft diameter, 44mm overall length; Item # 19007-14, Fine Science Tools (USA), Inc.) were made in the skull without damaging the dura and electrodes were secured to the skull using stainless steel screws (Plastics One, Part # 0-80X1/16, Internal control # 8L010121201F with shaft length=1.60 mm, head diameter=2.50 mm, shaft diameter=1.57 mm). EEG recording electrodes were placed at frontal cortex (AP +2.0, ML +2.0 mm), and parietal cortex (AP −6.0, ML +2.0 mm) and a ground electrode was placed in the midline over the cerebellum. An anchoring screw, without electrode, was placed ML −2.5 mm, at an equal distance between the coronal suture and the lambdoidal suture. Dental acrylic (Cat # 1255710; Henry Schein Inc, Indianapolis, IN; Lang Jet Denture Repair Acylic) was used to fix the electrode pedestal in place. Similar procedures were used for GAERS and NEC, except that rats were anaesthetized with isoflurane (0.8–1%), and implanted with gold plated screws (standard gold screw posts, Minerva Dental Limited, UK).

EEG recordings

Epileptic and nonepileptic animals were given a 1 week recovery period after surgery. For WAG/Rij and Wistar control rats, EEG signals were recorded via commutator (Plastics One, Inc.) using a Grass CP 511 amplifier (Grass- Telefactor, Astro Med, Inc., West Warwick, RI). Band pass frequency filter settings were 1–300 Hz. Signals were digitized at a sampling rate of 1 kHz with an NI USB-6008 A/D converter and LabView 7.1 software (National Instruments, Austin, TX), and analyzed using Spike 2 (Cambridge Electronic Design, Cambridge, UK). Similar recording procedures were used for GAERS and NEC except that signals were amplified using a Neurolog 104 differential amplifier (Digitimer, Welwyn Garden City, UK), digitally acquired and processed using pClamp 9 (Molecular Devices). For all animal groups, continuous EEG data were recorded for 3 hours from awake behaving rats between 10:00 a.m. and 5:00 p.m. Since even ordinary (unselected) Wistar rats can occasionally show a SWD phenotype (Coenen et al., 1992;Coenen and Van Luijtelaar, 2003), the non-epileptic control rats were screened by EEG and if significant SWD occurred, they were eliminated from the experiment. No selection procedure was used for the WAG/Rij, GAERS, or NEC rats.

Analysis of EEG data

SWDs were defined as large-amplitude (>2× the background EEG peak-to-peak amplitude) rhythmic 7–8 Hz discharges with typical spike-wave morphology lasting >1.0 s. Intervals containing artifact or slow wave sleep were excluded from the analysis. Start and end times for all SWDs were marked. Number of seizures, and seizure durations were then calculated. Percent time in SWD was determined as (sum of SWD interval durations/ total usable recording time) × 100% (Blumenfeld et al., 2008).

Intracardial perfusion of rats

Rats were anesthetized with sodium pentobarbital or Euthasol (100–150 mg/kg IP), followed by intracardiac perfusion with physiological NaCl solution and 4% cold paraformaldehyde (PFA) in 0.01M phosphate buffered saline (PBS) (pH = 7.4). After perfusion, brain was harvested maintaining integrity and stored in 4% PFA in PBS at 4 ° C. Before MRI, the brains were washed into PBS for 24h to remove the fixation solution and then, brain was placed into a custom-built MRI compatible tube. The tube was filled with Fluorinert, an MRI susceptibility-matching fluid (Sigma-Aldrich, Inc., St. Louis, MO).

MRI experiments

Imaging was conducted on a 9.4 T horizontal bore magnet (Bruker, Billerica, MA, U.S.A.) with a custom-made cosine ^{1}H radio frequency coil (14 mm diameter). A set of contiguous coronal slices were acquired to cover the entire brain. DTI experiments were performed using the Stejskal-Tanner spin-echo diffusion-weighted sequence using the following parameters, δ= 5 ms and Δ= 15 ms (where δ and Δ are the durations of diffusion gradient and time elapsed between the two diffusion gradients, respectively); repetition time (TR)/echo time (TE) = 1000/18 ms; the matrix size = 128 × 64, zero-filled to 256 × 128; number of averages was 28. The slice thickness was 0.5 mm, the in-plane resolution 230 μm × 230 μm. Fifteen images with noncollinear diffusion weighting with b = 1000 s/mm^2 were acquired along with one reference image with no diffusion weighting.

Image processing and analysis

The six independent elements of the diffusion tensor were calculated from each series of diffusion-weighted images. The resulting tensor element maps were used to derive the eigenvalues (λ1, λ2, and λ3) and the corresponding eigenvectors (e1, e2, e3) of the diffusion tensor by matrix diagonalization (Hasan et al., 2001;Jones et al., 1999). The DTI indices fractional anisotropy (FA), parallel diffusivity ($\lambda_{\|}$), and perpendicular diffusivity ($\lambda_{\perp}$) values were derived on a pixel-by-pixel basis using in house written software in Matlab (The MathWorks, Inc., Natick, MA) as defined by the following equations:

$$FA=\sqrt{\frac{3}{2}\frac{(\lambda_1-\lambda_{avg})^2+(\lambda_2-\lambda_{avg})^2+(\lambda_3-\lambda_{avg})^2}{\lambda_1^2+\lambda_2^2+\lambda_3^2}}$$

$$\lambda_{\|}=\lambda_1 \text{ and } \lambda_{\perp}=(\lambda 2+\lambda 3)/2$$

Image processing, ROI analyses and tractography were performed using BioImage Suite 2.6 (http://www.bioimagesuite.org/). FA maps were first manually coregistered to a common template by a rigid body transformation. The template for each group of animals was a dataset from a single animal within that group. To ensure that all slices retained the identical number of voxels for statistical analysis, any slices with missing data from the front or back of the brain following the rigid body transformation were eliminated. This step was followed by a non-linear intensity-based warping parameterized in terms of a tensor b-spline grid with uniform control point spacing (Papademetris et al., 2004). t-maps were generated from coregistered FA maps with t value threshold=2.00, extent threshold of 50 voxels (voxel dimensions = 0.234 × 0.234 × 0.5 mm) and FA threshold of 0.30. t-maps were then overlaid on the template FA maps for identification of regional changes, by comparison with a standard rat anatomical atlas (Paxinos and Watson, 1998). ROI analyses were performed by manually drawing ROIs in each individual image's original space before coregistration. The entire analysis was also confirmed using single ROIs in the common space, yielding the same results (data not shown). Two regions were identified for ROI analysis based on FA changes in the t-maps. 10 voxels were sampled across the body of the anterior corpus callosum near the midline at 1.3mm posterior to bregma and 10 voxels were sampled from each side of the superior fornix (20 voxels total) at 1.8mm posterior to bregma (see Supplementary Figure 1). Average FA, $\lambda_{\perp}$ and $\lambda_{\|}$ values within each ROI were then calculated, and statistical analysis performed comparing these values between matched groups of epileptic animals and nonepileptic controls.

We used tractography to verify that the selected ROIs were located in the expected anatomical white matter pathways. Tractography was performed using an eigenvector tracking algorithm

based on the fourth-order Runge-Kutta method (Basser et al., 2000). Fiber tracts were seeded from the same 10 voxels in the midline body of the anterior corpus callosum and 20 voxels in the superior fornix used in the ROI analysis (see Supplementary Figure 1). Fibers were restricted to regions with FA greater than 0.3 and maximum turning angle was limited to 45 degrees to prohibit biologically implausible tracts.

Results

EEG recordings confirmed frequent SWD in adult WAG/Rij and GAERS, but not in young WAG/Rij and not in controls. Mean SWD per hour were 18.21 ± 6.32 for adult WAG/Rij rats, and 54.83±30.92 for adult GAERS. The SWD per hour we observed were similar to those reported previously in these models of spike-wave epilepsy (Coenen et al., 1992;Coenen and Van Luijtelaar, 1987;Depaulis and van Luijtelaar, 2005). In contrast, mean SWD per hour were 0.38 ± 0.51 for adult nonepileptic Wistar controls, and no SWD were observed in young WAG/Rij rats, young nonepileptic Wistar controls, and in adult NEC rats. We also found that mean SWD duration and total time spent in SWD were increased in epileptic adult WAG/Rij and GAERS compared to young WAG/Rij and controls animals (see Table 1).

Adult WAG/Rij exhibited a strong localized decrease in FA in the anterior corpus callosum (AP −1.3 to −2.3 mm) compared to age-matched nonepileptic Wistar controls (Fig. 1). The decreased FA in the anterior corpus callosum was not seen in young WAG/Rij rats before the onset of SWD (Fig. 2). Other regions, such as the fornix also showed reduced FA in the WAG/Rij rats compared to controls. However, these differences were observed in WAG/Rij rats both before and after the onset of SWD (Fig. 1, Fig. 2), so they may reflect other strain differences not linked to the presence of SWD. To further test whether reduced FA in the anterior corpus callosum is related to the epileptic phenotype, we analyzed FA in GAERS, which have more severe SWD than WAG/Rij rats (Table 1). The GAERS exhibited a marked decrease in FA in the anterior corpus callosum, which was more extensive than in the WAG/Rij rats (Fig. 3). In comparing the GAERS to NEC, differences in FA in other regions such as the fornix were again seen. However, these were in the opposite direction from the WAG/Rij rats, with increased FA observed in the fornix of GAERS compared to NEC (Fig. 3). These data again suggest that FA differences in the fornix are not linked to the SWD phenotype.

To further quantify the changes in FA, ROI analyses were performed in the regions of the corpus callosum and fornix which showed the strongest differences. In the anterior corpus callosum, the FA values were decreased in adult epileptic WAG/Rij ($P<0.03$) and GAERS ($P<0.03$) compared to controls (Fig. 4 A). In contrast, the young WAG/Rij rats before the onset of SWD, experienced no significant FA differences in the anterior corpus callosum compared to controls (Fig. 4 A). The reduced fractional anisotropy seen in epileptic animals vs. control may indicate a loss in the density of axon fibers and myelin leading to increased perpendicular diffusivity ($\lambda\perp$); or a change in the individual axon fiber diameter leading to decreased parallel diffusivity ($\lambda\parallel$). Analysis of the full diffusion tensor including eigenvalues can provide information on structural integrity and the underlying histological processes following injury to cerebral white matter. With respect to $\lambda\perp$, the adult epileptic WAG/Rij ($P<0.003$) and GAERS ($P<0.03$) experienced significantly higher values in the corpus callosum compared to controls, with no significant difference between young WAG/Rij and controls (Fig. 4B). Investigation of $\lambda\parallel$ diffusivity parallel to the fibers in the corpus callosum showed no significant differences in young and adult WAG/Rij or GAERS compared to their controls (see Supplementary Figure 2 online). These findings suggest that reduced FA seen in the epileptic animals is due to an abnormal increase in $\lambda\perp$.

In the fornix, ROI analyses in both adult and young WAG/Rij rats exhibited reduced FA ($P<0.003$, $P<0.04$, respectively) compared to controls, and the GAERS had a significant

increase in the FA ($P<0.006$) compared to controls (Fig. 5A). In the fornix, $\lambda\perp$ the diffusivity perpendicular to the fibers, was significantly increased in adult and young WAG/Rij ($P<0.01$ and $P<0.05$, respectively) compared to controls while the GAERS exhibited a significant decrease in $\lambda\perp$ ($P<0.003$) compared to controls (Fig. 5 B). Like in the corpus callosum, there were no changes in $\lambda\parallel$ between any of the groups (see Supplementary Figure 2, online). As was already discussed, the changes in FA and $\lambda\perp$ in the fornix do not seem related to the presence of SWD, since both adult (epileptic) and young (before SWD onset) WAG/Rij rats showed similar changes in the fornix, while opposite changes were seen in epileptic GAERS.

We next used tractography to determine the anatomical course of the white matter pathways for all selected ROIs. In the example shown in Fig. 6, fiber tracts resulting from seeding the ROI in the anterior corpus callosum showed that the fibers interconnect the facial somatosensory cortex (S1BF) between the two hemispheres. The facial somatosensory cortex is known to be involved in seizure discharges in both WAG/Rij and GAERS (Meeren et al., 2002;Nersesyan et al., 2004b;Polack et al., 2007;Vergnes et al., 1990). Seeding the anterior corpus callosum ROI produced fiber tracts passing adjacent to S1BF bilaterally in 37 of 37 animals studied, and presumably interconnecting these regions. In addition, as expected, seeding the fornix ROIs (Fig. 6) led to fiber tracts passing to the bilateral hippocampi and hippocampal commissure in 37 of 37 animals studied.

Discussion

We found that DTI in rat models of absence epilepsy detected abnormal decreases in FA in the anterior corpus callosum. Adult epileptic WAG/Rij rats showed reduced callosal FA compared to controls, but these changes were not seen in young WAG/Rij rats before the onset of SWD. In addition, adult epileptic GAERS, which have a more severe SWD phenotype, had even more extensive FA changes in the anterior corpus callosum than the WAG/Rij rats. The reduced FA in epileptic animals was related to increased perpendicular diffusivity in the same regions, with no significant changes in parallel diffusivity. The area of anterior corpus callosum exhibiting these changes was shown through tractography to interconnect the bilateral facial somatosensory cortices, regions demonstrated previously to be involved in seizure discharges in the two hemispheres (Meeren et al., 2002;Nersesyan et al., 2004b).

These findings suggest that chronic abnormal epileptic activity in the cortex in spike-wave epilepsy may lead to microstructural changes in white matter pathways interconnecting the regions of seizure discharges. The functional consequences of these white matter changes are not known, and in fact it is not clear whether these changes are a consequence of SWD, or caused by some other aspect of the underlying disorder. However, we can speculate that chronic seizures cause white matter dysfunction in what has previously been considered mainly a gray matter disease, and that white matter dysfunction could contribute to some of the long-term attentional and other psychosocial problems seen in the generalized epilepsies (Camfield and Camfield, 2002;Wirrell et al., 1997). Decreased FA can be caused by decreased diffusivity parallel to axonal fibers or by increased perpendicular diffusivity (Beaulieu, 2002, 2006). Electron microscopy studies of reduced FA have related increased $\lambda\perp$ to reduced axons per cross-sectional area (Concha et al., 2008;Hui et al., 2007) or to decreased myelin (Gulani et al., 2001;Harsan et al., 2006). Reduced FA with decreased $\lambda\parallel$ has been related to reduced axonal caliber (Harsan et al., 2006;Wu et al., 2007). Since we saw reduced FA with increased $\lambda\perp$ and no significant change in $\lambda\parallel$ this suggests that these epilepsy models may have reduced axons or myelin in the affected white matter. Reduced FA with increased $\lambda\perp$ was also recently described in the fornix of temporal lobe epilepsy patients, and electron microscopy of excised tissue revealed increased extra-axonal fraction and reduced axonal density (Concha et al., 2008). Decreased FA with an increase in $\lambda\perp$ has also been observed in other conditions due to decreased myelin (Gulani et al., 2001;Harsan et al., 2006). Clearly, further studies with

electron microscopy will be necessary to determine the ultrastructural basis of the abnormalities in DTI that we observed in rodent SWD models.

Although epilepsy is usually not considered a white matter disease, several previous studies have suggested abnormalities in white matter and myelin as possible cause or effect of epilepsy. For example, as already discussed, DTI abnormalities have been found in patients and animal epilepsy models (Eriksson et al., 2001;Grant, 2005;Kimiwada et al., 2006;Luat and Chugani, 2008;Obenaus and Jacobs, 2007;Rugg-Gunn et al., 2001;Rugg-Gunn et al., 2002;Thivard et al., 2005). Epileptic seizures occur in several different rodent mutants with myelin diseases (Bloom et al., 2002;Bradl et al., 1999;Griffiths, 1996;Hoffmann et al., 2008;Rosenbluth, 1990;Seyfried et al., 1986). In humans, seizures are known to occur with increased incidence in patients with multiple sclerosis (Koch et al., 2008), and infantile spasm, a form of pediatric epilepsy, has been associated with abnormal myelination (Muroi et al., 1996;Schropp et al., 1994). Given our findings in rodent models, it will be of interest to determine if human patients with absence epilepsy have similar DTI abnormalities, and if these abnormalities occur in white matter pathways interconnecting the brain regions most intensely involved in absence seizures.

Although, as has already be mentioned, it is not known whether the DTI changes we observed were caused by seizures or by some other developmental change accompanying SWD, the animal models afford the opportunity to test whether SWD blockade can prevent the observed DTI changes. Early treatment of WAG/Rij rats with ethosuximide before the developmental onset of SWD and continued through adulthood was found to suppress seizures and molecular changes usually seen in these rats in adulthood even 3 months after the medication was stopped (Blumenfeld et al., 2008). Early treatment of GAERS for a shorter time period was found to have a similar, but somewhat less strong suppressive effect on SWD epileptogenesis (Dedeurwaerdere et al., 2005). It will be crucial in future studies to test whether early and sustained blockade of SWD in WAG/Rij and GAERS will be sufficient to prevent the observed DTI abnormalities. If these changes can be prevented by early therapy in rodent models, then DTI may be a promising biomarker for human therapeutic trials based on early treatment, once the genetic understanding of absence epilepsy allows presymptomatic diagnosis.

Our data suggest that DTI abnormalities in the corpus callosum were associated with SWD, as the changes were only seen in adult epileptic animals after the onset of seizures, and were more extensive in GAERS, which have a more severe SWD phenotype. The corpus callosum represents the most critical connection for the inter-hemispheric propagation of epileptic activity as it is the largest commissural fiber pathway, connecting cortical regions of the hemispheres. It has an essential role in the integration of information between the hemispheres (Gazzaniga, 2000), and has been shown previously to play a role in SWD synchrony (Musgrave and Gloor, 1980;Vergnes et al., 1989). Interestingly, a large degree of trans-hemispheric coherence was recently demonstrated between the right and left somatosensory cortex during SWDs in WAG/Rij rats (Sitnikova et al., 2006). We also observed decreased FA and increased $\lambda\perp$ in the fornix of WAG/Rij rats compared to controls. However, these changes were also present in young WAG/Rij rats before the onset of SWD, and the opposite changes (increased FA with decreased $\lambda\perp$) were seen in GAERS with robust SWD, suggesting that these changes in the fornix are not directly associated with the presence of SWD. Interestingly, the limbic circuitry including the hippocampus, which contributes major connections to the fornix, has been shown to be relatively spared during SWD in WAG/Rij and GAERS (Coenen and Van Luijtelaar, 2003;Nersesyan et al., 2004a;Vergnes et al., 1990). However, indirect evidence suggests altered limbic system function in these models, including increased resistance to kindling (Aker et al., 2006;Eskazan et al., 2002), and heightened anxiety and depression-like behaviors (Jones et al., 2008;Sarkisova et al., 2008). Therefore, the DTI changes we observed in the fornix may participate in as yet unknown mechanisms of altered limbic function in these models, not directly related to the presence of SWD. Ultimately, to determine whether the DTI

changes in the fornix are related in some way to SWD an important test will, again, be to investigate the effects of early treatment on the observed DTI changes.

In conclusion, we have found DTI abnormalities in the anterior corpus callosum in WAG/Rij rats and GAERS in the white matter pathway interconnecting bilateral cortical regions most directly involved in SWD. The abnormalities suggest that pathological changes occur in the white matter associated with this disorder, and may contribute to chronic or cumulative neurological abnormalities in absence epilepsy. Hopefully, with further investigation, DTI changes can become a useful noninvasive biomarker of absence epilepsy progression, and its prevention by early therapy.

Supplementary Material

Refer to Web version on PubMed Central for supplementary material.

Acknowledgements

This work was supported by NIH grants R01 NS-049307 (HB), R01 MH-067528, R01 DC-003710, P30 NS-52519 (FH), and by the Betsy and Jonathan Blattmachr family.

References

Aker RG, Yananli HR, Gurbanova AA, Ozkaynakci AE, Ates N, van Luijtelaar G, Onat FY. Amygdala kindling in the WAG/Rij rat model of absence epilepsy. Epilepsia 2006;47:33–40. [PubMed: 16417529]

Archer JS, Abbott DF, Waites AB, Jackson GD. fMRI "deactivation" of the posterior cingulate during generalized spike and wave. Neuroimage 2003;20:1915–1922. [PubMed: 14683697]

Assaf Y, Pasternak O. Diffusion tensor imaging (DTI)-based white matter mapping in brain research: a review. Journal of Molecular Neuroscience 2008;34:51–61. [PubMed: 18157658]

Avoli M, Gloor P. Interaction of cortex and thalamus in spike and wave discharges of feline generalized penicillin epilepsy. Experimental Neurology 1982;76:196–217. [PubMed: 7084360]

Avoli, M.; Gloor, P.; Kostopoulos, G.; Naquet, T., editors. Generalized Epilepsy. Boston: Birkhauser; 1990.

Basser PJ, Jones DK. Diffusion-tensor MRI: theory, experimental design and data analysis-a technical review. NMR Biomed 2002;15:456–467. [PubMed: 12489095]

Basser PJ, Pajevic S, Pierpaoli C, Duda J, Aldroubi A. In *vivo* fiber tractography using DT-MRI data. Magn Reson Med 2000;44:625–632. [PubMed: 11025519]

Beaulieu C. The basis of anisotropic water diffusion in the nervous system-a technical review. NMR Biomed 2002;15:435–455. [PubMed: 12489094]

Beaulieu, C. The biological basis of diffusion tractography; 2006 IEEE International Symposium on Biomedical Imaging; Virginia, USA: From Nano to Macro, Arlington; 2006. p. 347-350.

Berman R, Negishi M, Spann M, Chung M, Bai X, Purcaro M, Motelow JE, Dix-Cooper L, Enev M, Novotny EJ, Constable RT, Blumenfeld H. Simultaneous EEG, fMRI, and behavioral testing in typical childhood absence seizures. submitted. 2008

Bernasconi A, Bernasconi N, Natsume J, Antel SB, Andermann F, Arnold DL. Magnetic resonance spectroscopy and imaging of the thalamus in idiopathic generalized epilepsy. Brain 2003;126:2447–2454. [PubMed: 12902313]

Bloom CM, Anch AM, Dyche JS. Behavioral effects of chronic melatonin and pregnenolone injections in a myelin mutant rat (taiep). J Gen Psychol 2002;129:226–237. [PubMed: 12224808]

Blumenfeld H. From molecules to networks: cortical/subcortical interactions in the pathophysiology of idiopathic generalized epilepsy. Epilepsia 2003;44(Suppl 2):7–15. [PubMed: 12752456]

Blumenfeld H. Cellular and network mechanisms of spike-wave seizures. Epilepsia 2005;46(Suppl 9): 21–33. [PubMed: 16302873]

Blumenfeld H, Klein JP, Schridde U, Vestal M, Rice T, Khera DS, Bashyal C, Giblin K, Paul-Laughinghouse CP, Wang F, Phadke A, Mission J, Agarwal RK, Englot DJ, Motelow J, Nersesyan H, Waxman SG, Levin AR. Early treatment suppresses the development of spike-wave epilepsy in a rat model. Epilepsia 2008;49(3):400–409. [PubMed: 18070091]

Blumenfeld H, McCormick DA. Corticothalamic inputs control the pattern of activity generated in thalamocortical networks. Journal of Neuroscience 2000;20:5153–5162. [PubMed: 10864972]

Boska MD, Hasan KM, Kibuule D, Banerjee R, McIntyre E, Nelson JA, Hahn T, Gendelman HE, Mosley RL. Quantitative diffusion tensor imaging detects dopaminergic neuronal degeneration in a murine model of Parkinson's disease. Neurobiol Dis 2007;26:590–596. [PubMed: 17428671]

Bradl M, Bauer J, Inomata T, Zielasek J, Nave KA, Toyka K, Lassmann H, Wekerle H. Transgenic Lewis rats overexpressing the proteolipid protein gene: myelin degeneration and its effect on T cell-mediated experimental autoimmune encephalomyelitis. Acta Neuropathol 1999;97:595–606. [PubMed: 10378378]

Budde MD, Kim JH, Liang HF, Russell JH, Cross AH, Song SK. Axonal injury detected by in vivo diffusion tensor imaging correlates with neurological disability in a mouse model of multiple sclerosis. NMR Biomed. 2007

Camfield P, Camfield C. Epileptic syndromes in childhood: clinical features, outcomes, and treatment. Epilepsia 2002;43(Suppl 3):27–32. [PubMed: 12060004]

Chahboune H, Ment L, Stewart W, Ma X, Rothman D, Hyder F. Neurodevelopment of C57B/L6 mouse brain assessed by in *vivo* diffusion tensor imaging. NMR Biomed 2007;20:375–382. [PubMed: 17451176]

Chan CH, Briellmann RS, Pell GS, Scheffer IE, Abbott DF, Jackson GD. Thalamic atrophy in childhood absence epilepsy. Epilepsia 2006;47:399–405. [PubMed: 16499767]

Coenen AM, Drinkenburg WH, Inoue M, van Luijtelaar EL. Genetic models of absence epilepsy, with emphasis on the WAG/Rij strain of rats. Epilepsy Research 1992;12:75–86. [PubMed: 1396543]

Coenen AM, Van Luijtelaar EL. The WAG/Rij rat model for absence epilepsy: age and sex factors. Epilepsy Research 1987;1:297–301. [PubMed: 3143552]

Coenen AM, Van Luijtelaar EL. Genetic Animal Models for Absence Epilepsy: A Review of the WAG/Rij Strain of Rats. Behav Genet 2003;33:635–655. [PubMed: 14574120]

Concha L, Livy DJ, Gross DW, Wheatley BM, Beaulieu C. Direct correlation between diffusion tensor imaging and electron microscopy of the fornix in humans with temporal lobe epilepsy. Proc. Intl. Soc. Mag. Reson. Med. (ISMRM). 2008

Crunelli V, Leresche N. Childhood absence epilepsy: genes, channels, neurons and networks. Nature Reviews Neuroscience 2002;3:371–382.

Danober L, Deransart C, Depaulis A, Vergnes M, Marescaux C. Pathophysiological mechanisms of genetic absence epilepsy in the rat. Prog Neurobiol 1998;55:27–57. [PubMed: 9602499]

DeBoy CA, Zhang J, Dike S, Shats I, Jones M, Reich DS, Mori S, Nguyen T, Rothstein B, Miller RH, Griffin JT, Kerr DA, Calabresi PA. High resolution diffusion tensor imaging of axonal damage in focal inflammatory and demyelinating lesions in rat spinal cord. Brain 2007;130:2199–2210. [PubMed: 17557778]

Dedeurwaerdere S, Boon P, De Smedt T, Claeys P, Raedt R, Bosman T, Van Hese P, Van Maele G, Vonck K. Chronic levetiracetam treatment early in life decreases epileptiform events in young GAERS, but does not prevent the expression of spike and wave discharges during adulthood. Seizure 2005;14:403–411. [PubMed: 16095927]

Depaulis, A.; van Luijtelaar, EL. Genetic models of absence epilepsy in the rat. In: Pitkänen, A.; Schwartzkroin, PA.; Mosche, SL., editors. Models of seizures and epilepsy. London: Elsevier academic press; 2005. p. 233-248.

Duncan JS. Imaging idiopathic generalized epilepsy. Clinical EEG & Neuroscience. Official Journal of the EEG & Clinical Neuroscience Society (ENCS) 2004;35:168–172.

Duncan JS. Brain imaging in idiopathic generalized epilepsies. Epilepsia 2005;46(Suppl 9):108–111. [PubMed: 16302883]

Eriksson S, Rugg-Gunn F, Symms M, Barker G, Duncan J. Diffusion tensor imaging in patients with epilepsy and malformations of cortical development. Brain 2001;124:617–626. [PubMed: 11222460]

Eskazan E, Onat FY, Aker R, Oner G. Resistance to propagation of amygdaloid kindling seizures in rats with genetic absence epilepsy. Epilepsia 2002;43:1115–1119. [PubMed: 12366723]

Gazzaniga MS. Cerebral specialization and interhemispheric communication: does the corpus callosum enable the human condition? Brain 2000;123(Pt 7):1293–1326. [PubMed: 10869045]

Gotman J, Grova C, Bagshaw A, Kobayashi E, Aghakhani Y, Dubeau F. Generalized epileptic discharges show thalamocortical activation and suspension of the default state of the brain. Proceedings of the National Academy of Sciences of the United States of America 2005;102:15236–15240. [PubMed: 16217042]

Grant PE. Imaging the developing epileptic brain. Epilepsia 2005;46(Suppl 7):7–14. [PubMed: 16201990]

Griffiths IR. Myelin mutants: model systems for the study of normal and abnormal myelination. Bioessays 1996;18:789–797. [PubMed: 8885716]

Gulani V, Webb AG, Duncan ID, Lauterbur PC. Apparent diffusion tensor measurements in myelin-deficient rat spinal cords. Magnetic Resonance in Medicine 2001;45:191–195. [PubMed: 11180424]

Hamandi K, Laufs H, Nöth U, Carmichael DW, Duncan JS, Lemieux L. BOLD and perfusion changes during epileptic generalised spike wave activity. Neuroimage 2008;39:608–618. [PubMed: 17920297]

Harsan LA, Poulet P, Guignard B, Steibel J, Parizel N, de Sousa PL, Boehm N, Grucker D, Ghandour MS. Brain dysmyelination and recovery assessment by noninvasive in vivo diffusion tensor magnetic resonance imaging. J Neurosci Res 2006;83:392–402. [PubMed: 16397901]

Hasan KM, Basser PJ, Parker DL, Alexander AL. Analytical computation of the eigenvalues and eigenvectors in DT-MRI. J Magn Reson 2001;152:41–47. [PubMed: 11531362]

Hoffmann K, Lindner M, Groticke I, Stangel M, Loscher W. Epileptic seizures and hippocampal damage after cuprizone-induced demyelination in C57BL/6 mice. Exp Neurol 2008;210:308–321. [PubMed: 18096162]

Holmes MD, Brown M, Tucker DM. Are “generalized” seizures truly generalized? Evidence of localized mesial frontal and frontopolar discharges in absence. Epilepsia 2004;45:1568–1579. [PubMed: 15571515]

Hui, ES.; Fu, QL.; So, KF.; Wu, EX. Diffusion tensor MR study of optic nerve degeneration in glaucoma; Conf Proc IEEE Eng Med Biol Soc; 2007. p. 4312-4315.

ILAE. Proposal for revised clinical and electroencephalographic classification of epileptic seizures. From the Commission on Classification and Terminology of the International League Against Epilepsy. Epilepsia 1981;22:489–501. [PubMed: 6790275]

Jones DK, Horsfield MA, Simmons A. Optimal strategies for measuring diffusion in anisotropic systems by magnetic resonance imaging. Magn Reson Med 1999;42:515–525. [PubMed: 10467296]

Jones NC, Salzberg MR, Kumar G, Couper A, Morris MJ, O'Brien TJ. Elevated anxiety and depressive-like behavior in a rat model of genetic generalized epilepsy suggesting common causation. Experimental Neurology 2008;209:254–260. [PubMed: 18022621]

Kale RA, Gupta RK, Saraswat VA, Hasan KM, Trivedi R, Mishra AM, Ranjan P, Pandey CM, Narayana PA. Demonstration of interstitial cerebral edema with diffusion tensor MR imaging in type C hepatic encephalopathy. Hepatology 2006;43:698–706. [PubMed: 16557540]

Kim JH, Trinkaus K, Ozcan A, Budde MD, Song SK. Postmortem delay does not change regional diffusion anisotropy characteristics in mouse spinal cord white matter. NMR in Biomedicine 2007;20:352–359. [PubMed: 17451177]

Kimiwada T, Juhasz C, Makki M, Muzik O, Chugani DC, Asano E, Chugani HT. Hippocampal and thalamic diffusion abnormalities in children with temporal lobe epilepsy. Epilepsia 2006;47:167–175. [PubMed: 16417545]

Klein JP, Khera DS, Nersesyan H, Kimchi EY, Waxman SG, Blumenfeld H. Dysregulation of sodium channel expression in cortical neurons in a rodent model of absence epilepsy. Brain Research 2004;1000:102–109. [PubMed: 15053958]

Koch M, Uyttenboogaart M, Polman S, De Keyser J. Seizures in multiple sclerosis. Epilepsia 2008;49:948–953. [PubMed: 18336559]

Levav M, Mirsky AF, Herault J, Xiong L, Amir N, Andermann E. Familial association of neuropsychological traits in patients with generalized and partial seizure disorders. Journal of Clinical & Experimental Neuropsychology 2002;24:311–326. [PubMed: 11992214]

Luat AF, Chugani HT. Molecular and diffusion tensor imaging of epileptic networks. Epilepsia 2008;49 (Suppl 3):15–22. [PubMed: 18304252]

Meeren H, van Luijtelaar G, Lopes da Silva F, Coenen A. Evolving concepts on the pathophysiology of absence seizures: the cortical focus theory. Arch Neurol 2005;62:371–376. [PubMed: 15767501]

Meeren HK, Pijn JP, Van Luijtelaar EL, Coenen AM, Lopes da Silva FH. Cortical focus drives widespread corticothalamic networks during spontaneous absence seizures in rats. Journal of Neuroscience 2002;22:1480–1495. [PubMed: 11850474]

Mirsky AF, Van Buren JM. On the Nature of the "Absence" in Centrencephalic Epilepsy: A Study of some Behavioral, Electroencephalographic, and Autonomic Factors. Electroencephalogr Clin Neurophysiol 1965;18:334–348. [PubMed: 14267826]

Moeller F, Siebner HR, Wolff S, Muhle H, Granert O, Jansen O, Stephani U, Siniatchkin M. Simultaneous EEG-fMRI in drug-naive children with newly diagnosed absence epilepsy. Epilepsia Epub ahead of print. 2008

Mori S, Frederiksen K, van Zijl PC, Stieltjes B, Kraut MA, Solaiyappan M, Pomper MG. Brain white matter anatomy of tumor patients evaluated with diffusion tensor imaging. Annals of Neurology 2002;51:377–380. [PubMed: 11891834]

Mori S, Zhang J. Principles of diffusion tensor imaging and its applications to basic neuroscience research. Neuron 2006;51:527–539. [PubMed: 16950152]

Muroi J, Okuno T, Kuno C, Yorifuji T, Shimizu K, Matsumura M, Takahashi Y, Okuno T, Matsuo M. An MRI study of the myelination pattern in West syndrome. Brain Dev 1996;18:179–184. [PubMed: 8836497]

Musgrave J, Gloor P. The role of the corpus callosum in bilateral interhemispheric synchrony of spike and wave discharge in feline generalized penicillin epilepsy. Epilepsia 1980;21:369–378. [PubMed: 7398604]

Nersesyan H, Herman P, Erdogan E, Hyder F, Blumenfeld H. Relative changes in cerebral blood flow and neuronal activity in local microdomains during generalized seizures. J Cereb Blood Flow Metab 2004a;24:1057–1068. [PubMed: 15356426]

Nersesyan H, Hyder F, Rothman D, Blumenfeld H. Dynamic fMRI and EEG recordings during spike-wave seizures and generalized tonic-clonic seizures in WAG/Rij rats. J Cereb Blood Flow Metab 2004b;24:589–599. [PubMed: 15181366]

Obenaus A, Jacobs RE. Magnetic resonance imaging of functional anatomy: use for small animal epilepsy models. Epilepsia 2007;48(Suppl 4):11–17. [PubMed: 17767571]

Papademetris X, Staib LH, Jackowski AP, Win LY, Schultz RT, Duncan JS. Integrating intensity and feature nonrigid registration. Medical Image Computing and Computer-Assisted Intervention (MICCAI), LNCS 2004;3216(I):763–770.

Paxinos, G.; Watson, C. The rat brain in stereotaxic coordinates. Vol. 4th ed.. San Diego: Academic Press; 1998.

Polack PO, Guillemain I, Hu E, Deransart C, Depaulis A, Charpier S. Deep layer somatosensory cortical neurons initiate spike-and-wave discharges in a genetic model of absence seizures. Journal of Neuroscience 2007;27:6590–6599. [PubMed: 17567820]

Rodin E, Ancheta O. Cerebral electrical fields during petit mal absences. Electroencephalography & Clinical Neurophysiology 1987;66:457–466. [PubMed: 2438111]

Rosenbluth J. Axolemmal abnormalities in myelin mutants. Ann N Y Acad Sci 1990;605:194–214. [PubMed: 2268117]

Rugg-Gunn F, Eriksson S, Symms M, Barker G, Duncan J. Diffusion tensor imaging of cryptogenic and acquired partial epilepsies. Brain 2001;124:627–636. [PubMed: 11222461]

Rugg-Gunn FJ, Eriksson SH, Symms MR, Barker GJ, Thom M, Harkness W, Duncan JS. Diffusion tensor imaging in refractory epilepsy. Lancet 2002;359:1748–1751. [PubMed: 12049867]

Sarkisova KY, Kulikov MA, Midzyanovskaya IS, Folomkina AA. Dopamine-dependent nature of depression-like behavior in WAG/Rij rats with genetic absence epilepsy. Neuroscience & Behavioral Physiology 2008;38:119–128. [PubMed: 18197376]

Schropp C, Staudt M, Staudt F, Bise K, Obletter N, Breit A, Weinmann HM. Delayed myelination in children with West syndrome: an MRI-study. Neuropediatrics 1994;25:116–120. [PubMed: 7969793]

Seyfried TN, Glaser GH, Yu RK, Palayoor ST. Inherited convulsive disorders in mice. Adv Neurol 1986;44:115–133. [PubMed: 3518345]

Sitnikova E, van Luijtelaar G. Cortical and thalamic coherence during spike-wave seizures in WAG/Rij rats. Epilepsy Res 2006;71:159–180. [PubMed: 16879948]

Song SK, Kim JH, Lin SJ, Brendza RP, Holtzman DM. Diffusion tensor imaging detects age-dependent white matter changes in a transgenic mouse model with amyloid deposition. Neurobiol Dis 2004;15:640–647. [PubMed: 15056472]

Thivard L, Lehericy S, Krainik A, Adam C, Dormont D, Chiras J, Baulac M, Dupont S. Diffusion tensor imaging in medial temporal lobe epilepsy with hippocampal sclerosis. Neuroimage 2005;28:682–690. [PubMed: 16084113]

Vergnes M, Marescaux C, Depaulis A. Mapping of spontaneous spike and wave discharges in Wistar rats with genetic generalized non-convulsive epilepsy. Brain Research 1990;523:87–91. [PubMed: 2207693]

Vergnes M, Marescaux C, Lannes B, Depaulis A, Micheletti G, Warter JM. Interhemispheric desynchronization of spontaneous spike-wave discharges by corpus callosum transection in rats with petit mal-like epilepsy. Epilepsy Research 1989;4:8–13. [PubMed: 2502389]

Weir B. The morphology of the spike-wave complex. Electroencephalography & Clinical Neurophysiology 1965;19:284–290. [PubMed: 4157831]

Wirrell EC, Camfield CS, Camfield PR, Dooley JM, Gordon KE, Smith B. Long-term psychosocial outcome in typical absence epilepsy. Sometimes a wolf in sheeps' clothing. Archives of Pediatrics & Adolescent Medicine 1997;151:152–158. [PubMed: 9041870]

Woermann FG, Sisodiya SM, Free SL, Duncan JS. Quantitative MRI in patients with idiopathic generalized epilepsy. Evidence of widespread cerebral structural changes. Brain 1998;121:1661–1667. [PubMed: 9762955]

Wu Q, Butzkueven H, Gresle M, Kirchhoff F, Friedhuber A, Yang Q, Wang H, Fang K, Lei H, Egan GF, Kilpatrick TJ. MR diffusion changes correlate with ultra-structurally defined axonal degeneration in murine optic nerve. Neuroimage 2007;37:1138–1147. [PubMed: 17689104]

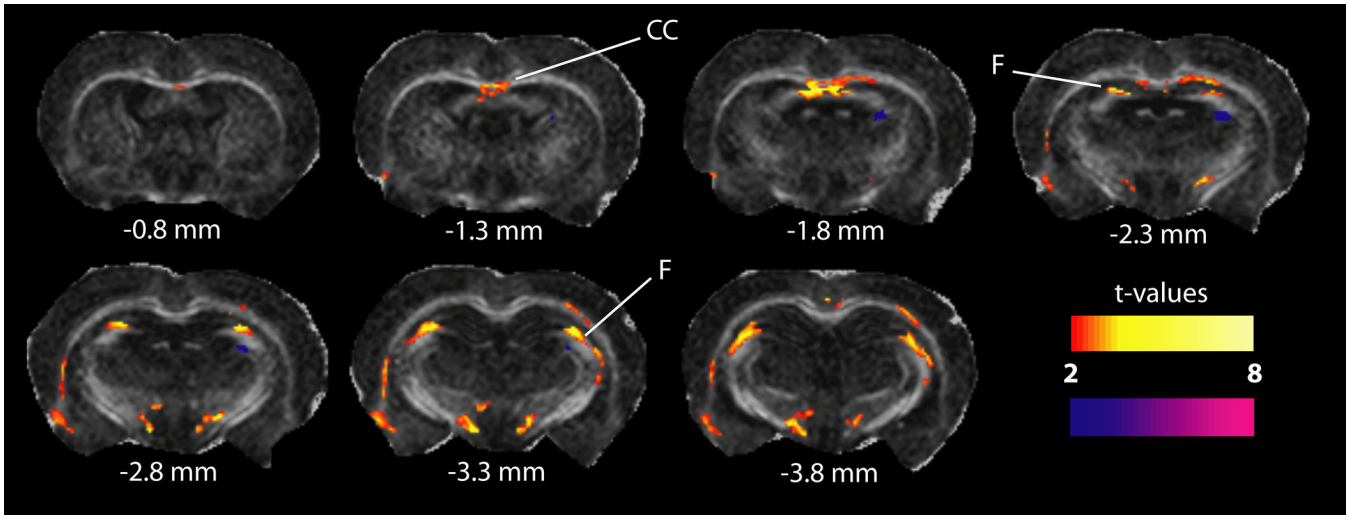

Figure 1.

Epileptic adult (8 mo) WAG/Rij rats have decreased fractional anisotropy in anterior corpus callosum and other regions compared to controls. t-maps from AP −0.8 to −3.8 mm are shown for adult WAG/Rij (n=9) vs.age-matched nonepileptic Wistar controls (n=7), with warm colors representing decreased FA in WAG/Rij vs. controls, and cool colors the opposite. In adult epileptic WAG/Rij rats, decreased FA was observed in the anterior corpus callosum (CC), and in other regions including the fornix (F). t value threshold=2.00, extent threshold = 50 voxels (voxel dimensions 0.234 × 0.234 × 0.5 mm), and FA threshold = 0.30.

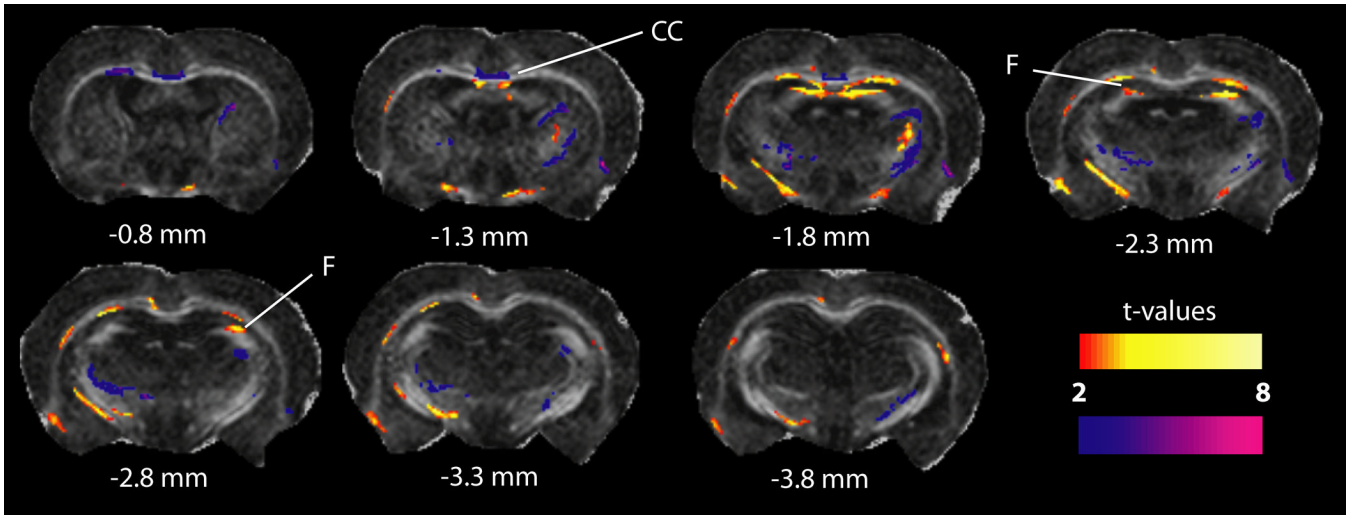

Figure 2.

Young (1.7 mo) WAG/Rij rats before onset of SWD do not have decreased fractional anisotropy in anterior corpus callosum. t-maps from AP −0.8 to −3.8 mm are shown for young WAG/Rij (n=6) vs. age-matched nonepileptic Wistar controls (n=5). Warm colors represent decreased FA in WAG/Rij vs. controls, and cool colors the opposite. Anterior corpus callosum (CC) does not show decreased FA in WAG/Rij vs. controls, while other regions including the fornix (F) do show decreases. t value threshold=2.00, extent threshold = 50 voxels (voxel dimensions 0.234 × 0.234 × 0.5 mm), and FA threshold = 0.30.

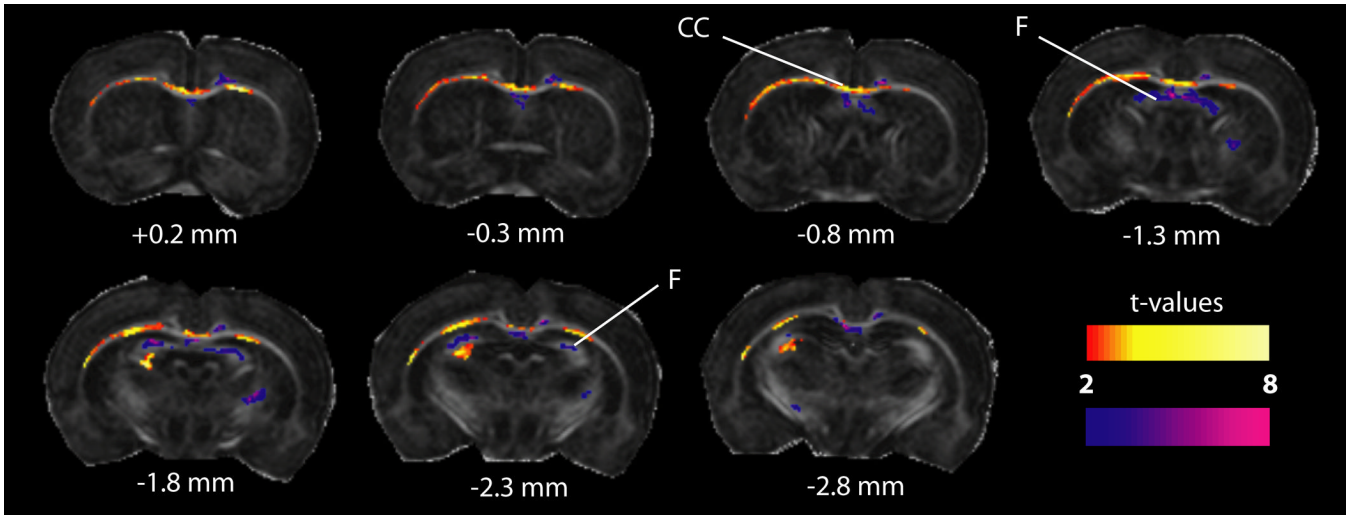

Figure 3.

Epileptic adult (4.2 mo) GAERS have decreased fractional anisotropy in anterior corpus callosum compared to nonepileptic controls. t-maps from AP +0.2 to −2.8 mm are shown for adult GAERS (n=5) vs. age-matched NEC (n=5). Warm colors represent decreased FA in GAERS vs. controls, and cool colors the opposite. In adult epileptic GAERS, extensive decreased FA was observed in the anterior corpus callosum (CC). Unlike the WAG/Rij rats (Figure 1, (Figure 2), the fornix (F) showed increased FA in GAERS vs. controls. t value threshold=2.00, extent threshold = 50 voxels (voxel dimensions 0.234 × 0.234 × 0.5 mm), and FA threshold = 0.30.

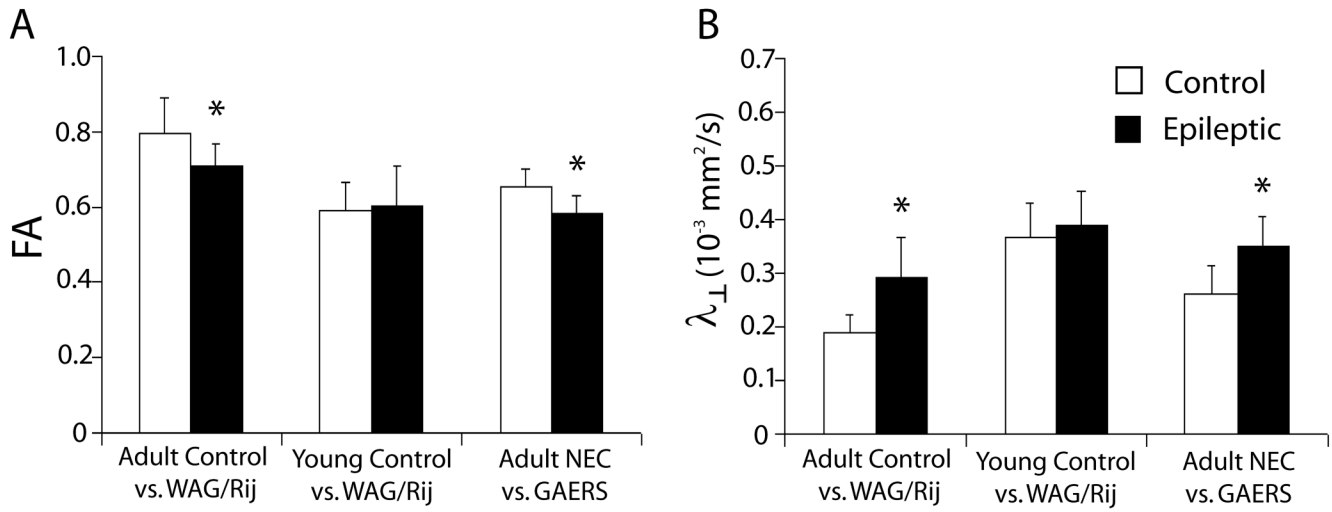

Figure 4.

Anterior corpus callosum shows reduced FA and increased perpendicular diffusivity ($\lambda_{\perp}$) in adult epileptic animals. **A.** FA values are decreased in adult WAG/Rij ($P<0.03$, two-tailed t-test) and GAERS ($P<0.03$) compared to controls. The young WAG/Rij experienced no significant FA differences in the anterior corpus callosum compared to controls. **B.** $\lambda_{\perp}$ was significantly higher in adult WAG/Rij ($P<0.003$) and GAERS ($P<0.03$) compared to control, with no significant difference between young WAG/Rij and controls. Animals and groups are the same as in Figure 1–Figure 3.

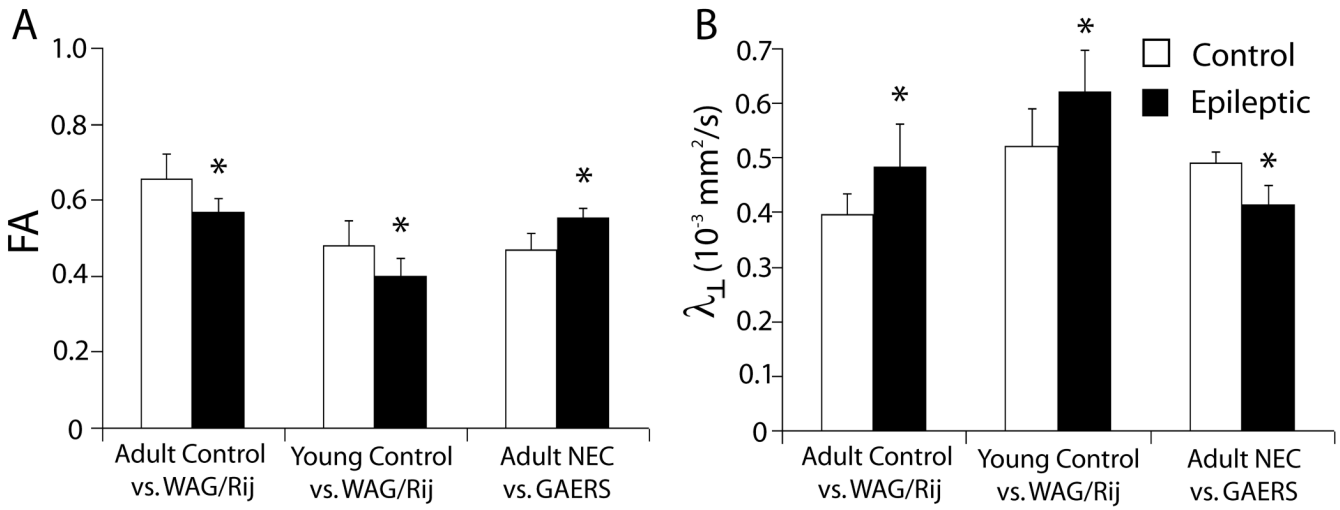

Figure 5.

Fornix shows reduced FA and increased λ⊥in adult and young WAG/Rij, but opposite changes in GAERS. **A.** Both adult and young WAG/Rij rats exhibit reduced FA ($P<0.003$, $P<0.04$, respectively; two-tailed t-test) compared to control, whereas the GAERS had significant increase in the FA ($P<0.006$) compared to control. **B.** Adult and young WAG/Rij exhibit a significant increase of $\lambda^{\perp}$ ($P<0.01$, $P<0.05$, respectively) compared to control, whereas the GAERS exhibit a significant decrease in $\lambda^{\perp}$ ($P<0.003$) compared to control. Animals and groups are the same as in Figure 1–Figure 3.

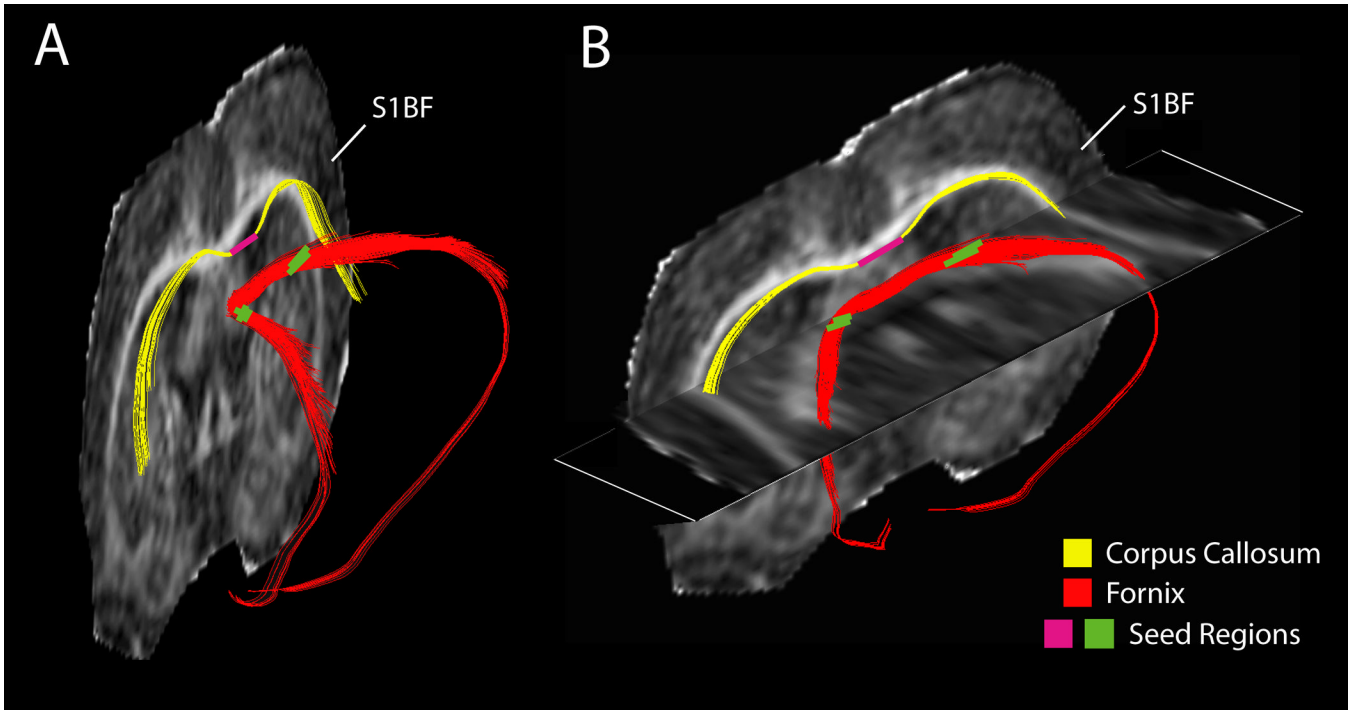

Figure 6.

Examples of tractography seeding from anterior corpus callosum and fornix ROIs. **A.** Oblique lateral view showing relationship between anterior corpus callosum ROI (purple) and fiber tracts (yellow) from this seed point leading to bilateral facial somatosensory cortex (S1BF). Seed points in bilateral fornix ROIs (green) lead to fiber tracts (red) in fornix that reach bilateral hippocampus (not shown) and hippocampal commissure. A single coronal FA map slice at AP −0.8 mm is shown for reference, along with the location of the barrel field primary somatosensory cortex (S1BF). **B.** Oblique superior view showing same tracts as in A. Coronal FA map slice at AP −0.8 mm and horizontal slice at SI 4.1mm relative to bregma are shown for reference.

Table 1

EEG analysis results for epileptic and nonepileptic animal groups[a]

Animal Group	SWD/hour	% time SWD	SWD duration (s)	N
Adult WAG/Rij	18.21 ± 6.32	1.92 ± 1.11	3.54 ± 1.06	9
Adult Wistar control	0.43 ± 0.52	0.02 ± 0.03	1.11 ± 1.06	7
Young WAG/Rij	0.00 ± 0.00	0.00 ± 0.00	0.00 ± 0.00	6
Young Wistar control	0.00 ± 0.00	0.00 ± 0.00	0.00 ± 0.00	5
Adult GAERS	54.83±30.92	14.28±10.96	10.04±9.35	5
Adult NEC	0.00 ± 0.00	0.00 ± 0.00	0.00 ± 0.00	5

[a] All values are mean ± SD.